Health State Estimation and Long-Term Durability Prediction for Vehicular PEM Fuel Cell Stacks Under Dynamic Operational Conditions

Xingwang Tang, Lei Shi, Ming Li, Sichuan Xu, and Chuanyu Sun, *Member, IEEE*

***Abstract*—To establish a reliable long-term estimation and prognosis for the state of health (SOH) and voltage degradation prediction of fuel cell stacks (FCSs), this article initiates a fusion prognostic strategy and a rolling prediction framework for long-term SOH estimation for FCSs based on the designed 2500-h prolonged durability experiment on vehicular FCS. Specifically, a time-varying dynamic degradation model is first developed to track the dynamic performance deterioration of FCSs based on the electrochemical mechanism and dynamic equivalent circuit model of the fuel cell. Subsequently, an improved Informer model is proposed for SOH estimation and voltage degradation prediction. The experimental results validate that the proposed model can effectively monitor the dynamic degradation behavior of the proton exchange membrane FCS, exhibiting superior accuracy in forecasting long-term voltage degradation. Moreover, the model can precisely predict the long-term aging trend and voltage periodic recovery of FCSs, with a root-mean-square error ranging from 0.33 to 1.04 V and a mean absolute percentage error below 0.5%. Finally, a rolling prediction framework for SOH estimation of FCSs, applicable to cloud-based implementation schemes, is developed to provide quantitative SOH estimation for each operational period, facilitating the development of FCS design and control strategies.**

***Index Terms*—Dynamic degradation models, long-term durability test, proton exchange membrane fuel cell stack, rolling prediction framework, state of health.**

I. Introduction

GREEN and low-carbon development has become the overarching trend in global energy evolution, with hydrogen energy emerging as the most promising secondary green energy source. As the key energy conversion devices within the hydrogen industry chain, fuel cell stacks (FCSs) play a pivotal role in the field of power electronics equipment such as fuel cell hybrid electric vehicles, fixed power systems, energy storage systems, mobile portable power devices, and drones [1], [2], [3], [4]. However, the lower lifetime of proton exchange membrane (PEM) fuel cells inhibits their widespread commercialization development [5], [6], [7]. Concerning the durability and reliability of fuel cell stacks (FCSs), current vehicular FCSs have a maximum service life of around 5000 h [8], while the expected life is at least 8000 h by 2025 for commercial low-duty automobiles [9], [10]. The primary factor contributing to the limited operational lifespan of fuel cells is the highly nonlinear degradation process of PEM fuel cells, encompassing multiple physical fields (heat transfer, mass transfer, two-phase flow, and electrochemistry), components (membrane electrode assembly, catalyst layer (CL), and gas diffusion layer), and factors (temperature, humidity, atmospheric pressure, external loads, and operating environment) [11], [12], [13]. During normal FCS operation, components experience irreversible degradation over time, resulting in a natural decline in performance. Furthermore, adverse operating conditions, such as the start-stop cycle, load-changing cycle, and thermal cycle cause issues like membrane thinning, ionic conductivity reduction, membrane pinhole and crack, and electrochemical surface area reduction. These undesirable phenomena further accelerate performance deterioration and, thus, affect the external characteristics.

The comprehensive examination of durability has become an important and pressing concern with the practical implementation of vehicular FCSs. The state of health (SOH) for fuel cells has a significant impact on the development of energy management strategies for vehicular FCSs [14], [15], [16], [17]. To overcome the challenge of low durability in PEM fuel cells and ensure their sustained and reliable performance throughout vehicle operating cycles, it is necessary to undertake essential management and system maintenance during fuel cell usage, including monitoring the SOH and predicting the future aging trend of FCSs. Therefore, prognostics and health management systems that can improve the durability of FCSs are considered to be superior solutions [18]. Within such a framework, the voltage degradation prediction or SOH of the PEM fuel cell can be predicted regularly. This proactive approach allows for the implementation of preventive maintenance based on the current SOH level, thereby mitigating irreversible degradations and prolonging the lifespan of fuel cells. Hence, investigating prognostic methods becomes significantly meaningful, aiming

Received 24 June 2024; revised 11 October 2024; accepted 11 November 2024. Date of publication 19 November 2024; date of current version 26 December 2024. This work was supported in part by the National Key R&D Program of China under Grant 2017YFB0102802 and in part by the State Scholarship Funding of CSC under Grant 202306260098. Recommended for publication by Associate Editor K. Gunawardane. *(Corresponding authors: Sichuan Xu; Chuanyu Sun.)*

Xingwang Tang, Lei Shi, and Sichuan Xu are with the School of Automotive Studies, Tongji University, Shanghai 201804, China (e-mail: tangxingwang@tongji.edu.cn; 2011681@tongji.edu.cn; scxu@tongji.edu.cn).

Ming Li is with the College of Automotive Engineering, Jilin University, Changchun 130025, China (e-mail: limingtiger@jlu.edu.cn).

Chuanyu Sun is with the School of Electrical Engineering and Automation, Harbin Institute of Technology, Harbin 150001, China (e-mail: chuanyu.sun@hit.edu.cn).

Color versions of one or more figures in this article are available at https://doi.org/10.1109/TPEL.2024.3502499.

Digital Object Identifier 10.1109/TPEL.2024.3502499

to enhance durability and reduce the development cost associated with FCSs.

Given the complexity of the vehicular FCS and the fact that the degradation mechanisms of fuel cells have not been entirely revealed until today, it is challenging to build accurate models to represent the deterioration phenomena of the PEM fuel cell. Many studies have been reported in this field to accurately characterize the current SOH level and future voltage degradation trend of FCSs [19], [20]. Prognostic methods for SOH estimation of FCSs can be broadly categorized as model-based, data-based, and hybrid methods [21], [22], [23]. The model-based method predicts the degradation rate based on the empirical or physical models of the FCS. Ou et al. [25] combined the Unscented Kalman filter with three kinds of empirical degradation models to explore the degradation behavior of FCSs and proposed a model-driven lifespan prediction method. The model is verified using the experimental data of fuel cell vehicles performing mail service on real roads, revealing that the method can be applied to the degradation trend prediction under real conditions. Ou et al. [25] proposed a semiempirical model based on the polarization behavior of FCSs and introduced the electrochemical surface area (ECSA) decay model and equivalent resistance model to predict the future decline trend of fuel cells. In addition, recovery factors are also introduced into the model to characterize the performance recovery of PEM fuel cells after start-up and shutdown. Futter et al. [26] established a two-dimensional (2-D) physical model of FCSs to simulate the chemical degradation processes of the PEM and verified the correctness of the degradation model through experimental data obtained by Accelerated Stress Test. Results show that the model can effectively predict the decay rate of the PEM under varying working pressures, humidity levels, and voltages. While empirical models or semiempirical models can predict the future aging trend of fuel cells to a certain extent and simplify the modeling process, PEM fuel cell stacks present challenges due to their complex nature as highly multiphysics, multiscale, and interplayed nonlinear characteristics. This complexity results in unclear degradation mechanisms, making it challenging to fully capture the aging behavior and related model parameters through model-based methods. With that being said, current model-based methods cannot meet the commercialization requirements in terms of accurately assessing the aging behavior of FCSs.

Compared with model-based prediction methods, data-driven prediction methods do not need to analyze the internal decay mechanisms of fuel cells [27]; the method learns the decay behavior of FCSs from the aging experimental data through machine learning or deep learning models, which can usually achieve high prediction accuracy. The combination of deep neural networks and PEM fuel cell prognostics has recently expressed a broad research perspective. The deep-learning-based methods, such as the convolutional neural network [28], [29], echo state network [30], [31], and recurrent neural network family methods [32], [33], have been well studied by many researchers and have shown satisfactory performance in degradation prediction. Lv et al. [34] proposed a Transformer-based prognostic framework with the series-attention mechanism to predict the degradation of the fuel cell and uses the relative voltage-loss rate as a health indicator in this model. The result shows that the proposed algorithm exhibits advantages in long-term prognostic, but with the further extension of the prediction horizon, the prognostic performance is hard to guarantee. Pan et al. [35] divided the degradation trend of fuel cells into reversible decay and irreversible decay and used the adaptive Kalman filter algorithm and nonlinear autoregressive with the exogenous model to extract and predict the information of irreversible decay and reversible decay, respectively. The prediction results show that the method has good prediction ability. To sum up, although data-driven methods have achieved good prediction results, especially under steady-state conditions, long-term SOH estimation, or degradation prediction of FCSs under dynamic load conditions is still challenging.

In addition, some scholars combined the advantages of model-based prediction methods and data-driven prediction methods and proposed a hybrid method to predict the degradation of PEM fuel cells in the early stage [36], [37]. Generally, the hybrid method can be subdivided into three types [38], [39], [40].

1) The model-based method is used to extract the degradation features of the PEM fuel cell, and then use the data-driven method to predict the degradation trend and estimate SOH.
2) The degradation model or measured data is fitted based on the data-driven method, and then the model-based method is used to predict degradation trends.
3) The degradation prediction is implemented using two or more model-based and data-driven methods, and each result is weighted and summed to obtain the final estimation result of SOH.

Based on a comprehensive review of the long-term estimation and prognostic for vehicular FCSs, it is evident that while some researchers have conducted extensive research on how to estimate the current SOH and predict the degradation trend accurately, significant challenges persist in this domain. These challenges are particularly pronounced in the context of vehicular FCSs, including the scarcity of long-term durability data and the need for credible long-term prognostic of fuel cell lifetime. Besides, a more significant challenge is that the polarization characteristics of FCSs during the degradation process cannot be obtained by existing methods. Moreover, these methods are based on extracting the voltage of the fuel cell at a certain current offline to estimate its health state. However, when the FCS is operated under dynamic cycles, the current is constantly changing, and it is difficult to obtain the voltage at a certain current continuously. To tackle the above challenges and problems, this article proposes a fusion prognostic strategy and a rolling prediction framework for long-term degradation prediction for FCSs based on the designed 2500-h long-term durability experiment. In comparison to existing literature, the novelties and contributions of this study can be summarized as follows.

1) A complete durability experiment of the vehicular FCS is designed, and the corresponding long-term degradation characterization data of the vehicular FCS under the dynamic operation scenario is collected.
2) A time-varying dynamic degradation model is developed to track the dynamic performance deterioration of FCSs

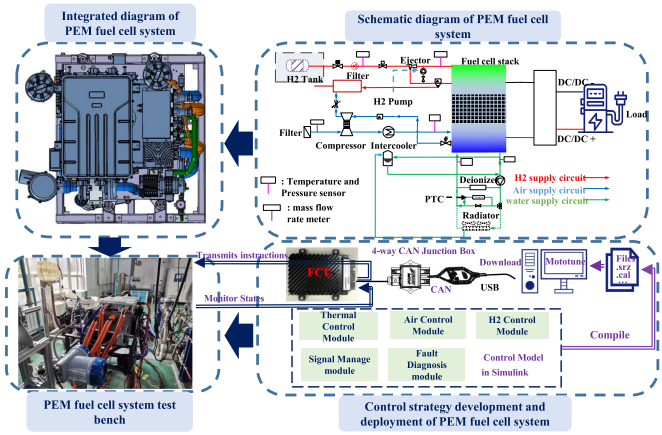

Fig. 1. Schematic diagram of the FCS and durability test platform.

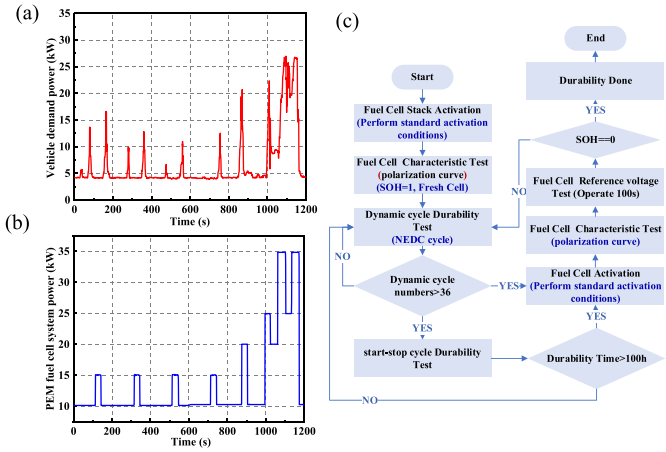

Fig. 2. Designed durability test scheme. (a) Passenger vehicle power demand. (b) Durability test dynamic cycle. (c) Test protocol.

TABLE I
BASIC TECHNICAL PARAMETERS OF PEMFC SINGLE CELL

Technical parameters	Values
Voltage range	210–365 V
Current range	0–400 A
Rated voltage	230 V
Rated current	295 A
Anode gas pressure	10–150 kPa
Cathode gas pressure	30–170 kPa
Maximum power	85 kW
Operation Temperature	–40 °C–90 °C

based on the electrochemical mechanism and dynamic equivalent circuit model (ECM) of the fuel cell.

3) A fusion prognostic strategy using the improved Informer model and time-varying degradation model is first provided to make a credible long-term estimation and prognostic for vehicular fuel cell stacks.
4) A rolling framework for SOH estimation, applicable to cloud-based implementation schemes, is developed to provide quantitative SOH estimation for each operational period, facilitating the development of FCS design and control strategies.

II. EXPERIMENT SETUP OF FUEL CELLS DURABILITY DATASET

As depicted in Fig. 1, the 85 kW vehicular FCS employs a durability test system, including some other necessary accessories such as the air subsystem, hydrogen subsystem, thermal management subsystem, electrical subsystem, control module, and fuel cell stack module (refer to Table I for detailed parameters). The experiment control platform mainly includes the upper computer (UP), the rapid control prototype (RCP) controller (Woodward MotoHawk SECM-112) with the 32-bit Freescale MPC564xA microprocessor, and the CAN-USB Bus Analyzer (Kvaser). Before the experiments, the controller codes in Simulink are compiled via MATLAB/Simulink RTW and then downloaded into the RCP controller using the software MotoTune. During durability testing, the UP software and Kvaser toolkit are applied to transmit the controller instructions and monitor various system operation states in real time. Besides, the operating parameters of the vehicular fuel cell stack at each power are determined according to the optimal working conditions provided by the manufacturer.

To verify the reliability of the proposed lifespan prediction method for vehicular FCSs, a dynamic operation cycle tailored to match the actual power output of fuel cell hybrid electric vehicles is devised, as shown in Fig. 2. The durability dynamic cycle includes idling, low, medium, and high load stages of vehicle operation, each lasting 1200 s, with a maximum load-up rate of 20 A/s and a maximum load-down rate of 30 A/s. In this durability performance test protocol, 7526 cycles are performed over a period of 2500 h. Notably, after every 36 cycles, a shutdown procedure is performed to simulate the effect of the start-stop cycle on fuel cell degradation. During the test, the polarization curve and reference voltage (voltage at the reference current of 102 A) are measured every 100 h to evaluate the performance of the vehicular FCS. After obtaining the current degradation voltage data of the vehicular FCS, the improved singular spectrum analysis method is used to eliminate the noise existing in the original data to enhance the effective degradation characteristic information of the obtained fuel cell voltage data. The improved singular spectrum analysis methods can refer to the previously published article [23].

III. DYNAMIC DEGRADATION MODEL OF PEMFCS

The voltage of the fuel cell is an important parameter to characterize the degradation trend. According to Chinese National Standard [41] (GB/T38914-2020), the fuel cell degradation trend is the change in cell voltage corresponding to the same reference current, where the reference current is the current at an average cell voltage of 0.7 V when the fuel cell is first used. During normal operation of the fuel cell, the voltage is affected by factors such as hydrogen and air pressure, concentration,

temperature, and so on [42], [43]. In general, the output voltage of fuel cells consists of four components, which are open voltage E_{ocv}, activation loss V_{act}, ohmic loss V_{ohm}, and concentration loss V_{conc}. The typical polarization curve model can be characterized as

$$E_{\text{cell}}^{\text{static}} = E_{\text{ocv}} - V_{\text{act}} - V_{\text{ohm}} - V_{\text{conc}} \tag{1}$$

$$E_{\text{nernst}} = 1.229 - 0.85 \times 10^{-3}\left(T_{\text{cell}} - 298.15\right) + 4.3085 \times 10^{-5} T_{\text{cell}}\left[\ln\left(P_{\text{H}_2}\right) + 0.5\ln\left(P_{O_2}\right)\right] \tag{2}$$

$$E_{\text{ocv}}^{\text{static}} = E_{\text{nernst}} - \frac{RT}{zF}\ln\left(\frac{j_{\text{loss}}}{j_0}\right) \tag{3}$$

$$\begin{cases} V_{\text{act}} = \frac{RT_{\text{stack}}}{2\xi_a \text{F}}\ln\left(\frac{j_{\text{cell}}+j_{\text{loss}}}{j_0}\right) \\ V_{\text{ohm}} = R_r \cdot j_{\text{stack}} \\ V_{\text{conc}} = k_c \frac{RT_{\text{stack}}}{4\xi_c \cdot \text{F}} \cdot \ln\left(1 - \frac{j_{\text{cell}}}{j_{\text{lim}}}\right) \end{cases} \tag{4}$$

where j_{stack} is the current density, j_0 is the exchange current density, j_{loss} is the crossover current density, j_{lim} is the limiting current density, k_c is the concentration losses coefficient, ξ is the charge transfer coefficient, and T_{cell} is the operating temperature of the fuel cell.

However, (2)–(4) are generally applicable to describe the voltage response of fuel cells under static operating conditions [44], but it is inadequate for capturing the transient voltage evolutions under dynamic conditions, making it unsuitable for characterizing the dynamic changes in fuel cells during vehicle operating cycles. In general, PEM fuel cells exhibit a fast dynamic behavior during operation, which is known as the "double charge layer" phenomenon [45]. Since electron transport is more rapid than gas mass transfer, when the load current changes dynamically, the increase or disappearance of charge will have a certain time delay, which will affect the activation and concentration polarization. Therefore, there is a time delay for the activation and concentration potentials, and then the voltage will change dynamically with the current (voltage undershoot) until reaching new steady-state values. To characterize the dynamic degradation behavior of PEM fuel cells under dynamic driving cycles, particularly focusing on the "double charge layer" phenomenon during sudden voltage changes, the dynamic output voltage of the fuel cell, including steady-state voltage and changing-load voltage, can be defined by the (5), and the corresponding time-varying dynamic degradation model of the fuel cell under the vehicular cycle is shown in Fig. 3. The output voltage of the fuel cell under dynamic cycle can be written as (6)

$$\begin{cases} E_{\text{cell}}^{\text{static}} = E_{\text{ocv}}^{\text{static}} - V_{\text{act}} - V_{\text{ohm}} - V_{\text{conc}} & \Delta j_{\text{cell}} < \Delta j_{\text{cell}}^{\text{lim}} \\ \begin{cases} U_{\text{dyn}} = E_{\text{ocv}} - U_1 - I_{\text{t}} R_{\text{r}} \\ U_1 = I_{\text{t}} R_{\text{equal}}\left(1 - e^{-\frac{t}{R_{\text{equal}} C_{\text{dl}}}}\right) \\ R_{\text{equal}} = R_{\text{ct}} + R_{\text{mt}}\left(1 - e^{-\frac{t}{R_{\text{mt}} C_1}}\right) \end{cases} & \Delta j_{\text{cell}} \geq \Delta j_{\text{cell}}^{\text{lim}} \end{cases} \tag{5}$$

$$\text{E}_{\text{cell}}^{\text{dyn}} = concat(E_{\text{cell}}^{\text{static}}, U_{\text{dyn}}) \tag{6}$$

where R_{ct} and R_{mt} are used to model the activation and concentration voltage polarization caused by charge transport and mass transport under sudden voltage change. *concat* is a function

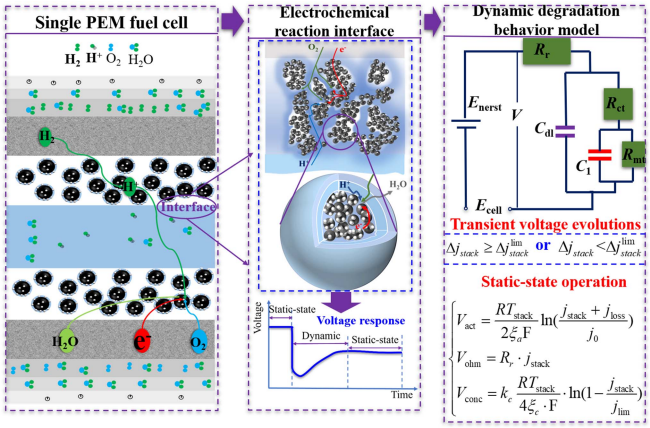

Fig. 3. Time-varying dynamic degradation model of the fuel cell.

that concatenates two pieces of data, $\Delta j_{\text{stack}}^{\text{lim}}$ is defined as the maximum current loading amplitude according to the study by Spicgel et al. [46]. This value can be viewed as the critical point at which the fuel cell is free of gas starvation under the load-switching moments, as calculated by

$$\Delta j_{stack}^{\text{lim}} = zF\frac{c_2 - c_1}{\left(\frac{1}{h_m} + \frac{\delta}{D^{eff}}\right)} \tag{7}$$

where h_m is the fluid transfer coefficient, D^{eff} is the effective diffusion coefficient, δ is the thickness of the gas diffusion layer, and c is the gas concentration in the flow channel.

As shown in Fig. 3 and (5), when a fuel cell is operating under dynamic operating conditions, according to the relationship between Δj_{cell} and $\Delta j_{\text{cell}}^{\text{lim}}$, the actual operation cycle can be divided into steady-state and changing-load operations. The dynamic degradation behavior of the PEM fuel cell under the load-switching moments can be represented by an ECM, where the polarization loss associated with internal physical processes along the electrode surface is characterized by resistors and capacitors. In this model, the resistor R_{r} is used to quantify the proton transfer loss corresponding to ohmic losses; R_{ct} and R_{mt} are used to model the activation and concentration voltage polarization caused by charge transport and mass transport under the sudden voltage change; the capacitor C_{dl} indicates the charge storage at the cathode-electrolyte interface. In order to identify the time-varying dynamic characteristic of the fuel cell under dynamic operating conditions, especially at the moment of load switching, a frequency domain mathematical expression based on the equivalent circuit model in Fig. 3 can be given by

$$U_{\text{dyn}}(s) = E_{\text{ocv}}(s) - i_{\text{t}}(s)\left(R_{\text{r}} + \frac{R_{\text{ct}} + \frac{R_{\text{mt}}}{1+R_{\text{mt}}C_1 s}}{R_{\text{ct}}C_{dl}s + \frac{R_{\text{mt}}C_{dl}s}{1+R_{\text{mt}}C_1 s} + 1}\right). \tag{8}$$

So the transfer function can be written as follows:

$$G(s) = \frac{U_{\text{dyn}}(s) - E_{\text{ocv}}(s)}{i_{\text{t}}(s)} = -\left(R_{\text{r}} + \frac{R_{\text{ct}} + \frac{R_{\text{mt}}}{1+R_{\text{mt}}C_1 s}}{R_{\text{ct}}C_{dl}s + \frac{R_{\text{mt}}C_{dl}s}{1+R_{\text{mt}}C_1 s} + 1}\right). \tag{9}$$

Let $s = \frac{2}{\Delta t}\frac{1-z^{-1}}{1+z^{-1}}$, (9) can be rewritten as follows:

$$G(z^{-1}) = \frac{B(z^{-1})}{A(z^{-1})} = \frac{b_0 + b_1 z^{-1} + b_2 z^{-2}}{1 + a_1 z^{-1} + a_2 z^{-2}} \tag{10}$$

where z^{-1} is the unit back-shift operator.

Let $V_{\mathrm{f}} = U_{\mathrm{dyn}} - E_{\mathrm{ocv}}$, (10) can be written as follows:

$$v_{\mathrm{f}}(k) = \frac{B(z^{-1})}{A(z^{-1})} i_{\mathrm{t}}(k). \tag{11}$$

Thus, (11) can be rewritten as follows:

$$v_{\mathrm{f}}(k) = (1 - A(z^{-1}))v_{\mathrm{f}}(k) + B(z^{-1})i_{\mathrm{t}}(k). \tag{12}$$

According to (10) and (12), (12) can be expressed as

$$\begin{aligned} v_f(k) = & -a_1 v_f(k-1) - a_2 v_f(k-2) + b_0 i_{\mathrm{t}}(k) \\ & + b_1 i_{\mathrm{t}}(k-1) + b_2 i_{\mathrm{t}}(k-2). \end{aligned} \tag{13}$$

Equation (13) can be written as

$$\begin{aligned} V_f(k) = & -\theta_1 V_f(k-1) - \theta_2 V_f(k-2) + \theta_3 i_t(k) \\ & + \theta_4 i_t(k-1) + \theta_5 i_t(k-2) \\ = & \Phi_k \cdot \Theta_k^T + \varepsilon(k) \end{aligned} \tag{14}$$

where $\varepsilon(k)$is the parameter estimation error; Φ_k andΘ_k can be written, respectively, as follows:

$$\Phi_k = \begin{bmatrix} -V_f(k-1) & -V_f(k-2) & i_t(k) & i_t(k-1) & i_t(k-2) \end{bmatrix} \tag{15}$$

$$\Theta_k = \begin{bmatrix} \theta_1 & \theta_2 & \theta_3 & \theta_4 & \theta_5 \end{bmatrix}. \tag{16}$$

In order to solve the parameters estimation vector Θ_k, the extended kernel iterative recursive least-squares algorithm is applied to minimize the cost function in this article, as follows:

$$l_{\mathrm{loss}} = \frac{1}{N}\sum_{k=1}^{N}\left(v_f(k) - \Phi_k \cdot \Theta_k^T\right)^2 \tag{17}$$

where N is the length of the data window.

When feeding the data of both temporal input $i_t(t)$ and output U_{dyn} of the fuel cell under dynamic operating conditions, Θ_k can be obtained.

Furthermore, according to (10), let

$$\begin{cases} m_1 = R_{\mathrm{ct}} C_{dl} R_{\mathrm{mt}} C_1 \\ m_2 = R_{\mathrm{ct}} C_{dl} + R_{\mathrm{mt}} C_1 + R_{\mathrm{mt}} C_{dl} \\ m_3 = R_{\mathrm{r}} R_{\mathrm{ct}} C_{dl} R_{\mathrm{mt}} C_1 \\ m_4 = R_{\mathrm{r}} R_{\mathrm{ct}} C_{dl} + R_{\mathrm{r}} R_{\mathrm{mt}} C_1 + R_{\mathrm{r}} R_{\mathrm{mt}} C_{dl} + R_{\mathrm{ct}} R_{\mathrm{mt}} C_1 \\ m_5 = R_{\mathrm{r}} + R_{\mathrm{ct}} + R_{\mathrm{mt}} \end{cases}, \text{ the}$$

relationship between Θ_k, and dynamic degradation characteristic parameters R_{r}, R_{ct}, C_{dl}, C_1, and R_{mt} can be expressed as

$$\begin{bmatrix} 4\theta_5 & 2\theta_5\Delta t & -4 & 2\Delta t & -\Delta t^2 \\ 4\theta_4 & 2\theta_4\Delta t & 8 & 0 & -2\Delta t^2 \\ 4\theta_3 & 2\theta_3\Delta t & -4 & -2\Delta t & -\Delta t^2 \\ 4\theta_2 + 4 & 2(\theta_2 - 1)\Delta t & 0 & 0 & 0 \\ 4\theta_1 - 8 & 2\theta_1\Delta t & 0 & 0 & 0 \end{bmatrix} \begin{bmatrix} m_1 \\ m_2 \\ m_3 \\ m_4 \\ m_5 \end{bmatrix}$$

$$= \begin{bmatrix} -\Delta t^2\theta_5 \\ -\Delta t^2\theta_4 \\ -\Delta t^2\theta_3 \\ -\Delta t^2\theta_2 - \Delta t^2 \\ -\Delta t^2\theta_1 - 2\Delta t^2 \end{bmatrix}. \tag{18}$$

Based on the (18), $[m_1, m_2, m_3, m_4, m_5]$ can be easily solved. So the dynamic degradation characteristic R_r, R_{ct}, C_{dl}, and R_{mt} can be further obtained.

Besides, according to (4), to accurately characterize the voltage variation of fuel cells under dynamic cycling, j_{loss}, j_{lim}, and j_0 need to be further calculated. Specifically, j_{lim} is related to the effective diffusion coefficient of oxygen $D_{\mathrm{O_2}}^{\mathrm{eff}}$, the thickness of the gas diffusion layer δ, and the reactant concentration c_R^0 in the cathode gas channel. Hence, j_{lim} can be expressed as

$$j_{\mathrm{lim}} = nFD_{\mathrm{O_2}}^{\mathrm{eff}}\frac{c_R^0}{\delta}. \tag{19}$$

Moreover, the relationship between j_{lim} and the durability time can satisfy the following equation:

$$j_{\mathrm{lim}}(t) = e^{\left(d_1 + d_2 \cdot t + d_3 \cdot t^2\right)|} \tag{20}$$

where d_1, d_2, and d_3 is the decay factor of the j_{lim}, which can be obtained by limiting current density measurement.

In this article, to calibrate the decay coefficient of the j_{lim}, the limiting-current measurement is performed before the durability cycle test, after the completion of the durability cycle of 250 h, and after the completion of the entire durability cycle. Specifically, the gases are introduced into the fuel cell through a humidifier with dry-gas flow rates of 500 and 650 cm^3/min for H_2 and diluted O_2 (1% O_2 in balance N_2), respectively. Typical operating conditions of fuel cells are 150 kPa total gas pressure, 80 °C, and 90% RH. At each specified condition, a polarization curve is measured by sweeping the potential from the open circuit to 0.15 V at a 5 mV/s scan rate. In the resulting curve, the largest current is employed as the limiting current density.

Meanwhile, j_0 is related to the ECSA of the CL, and the high potential is the main reason for the reduction of ECSA during fuel cell durability testing, j_0 can be expressed as

$$j_0 = \frac{j_{\mathrm{loss}}}{e^{(E_{\mathrm{nernst}} - \mathrm{OCV})\frac{zF}{RT}}} \tag{21}$$

where OCV is the open circuit voltage, which can be easily acquired during the durability test.

In addition, j_{loss} denotes the hydrogen crossover current density, which is usually caused by the crossover between hydrogen and air. In general, the change in the hydrogen crossover current is very small and almost constant over a long period. However, the j_{loss} increases rapidly in the later stage, which leads to the nonlinear deterioration of the fuel cell lifespan. Therefore j_{loss}can be expressed as follows:

$$j_{\mathrm{loss}} = j_{\mathrm{loss},0} \times e^{b_{\mathrm{loss}}t}. \tag{22}$$

Therefore, once dynamic degradation characteristic parameters R_{r}, R_{ct}, C_{dl}, C_1, R_{mt}, j_{loss}, j_{lim}, and $j_0$can be accurately identified, the electrochemical mechanism-based degradation

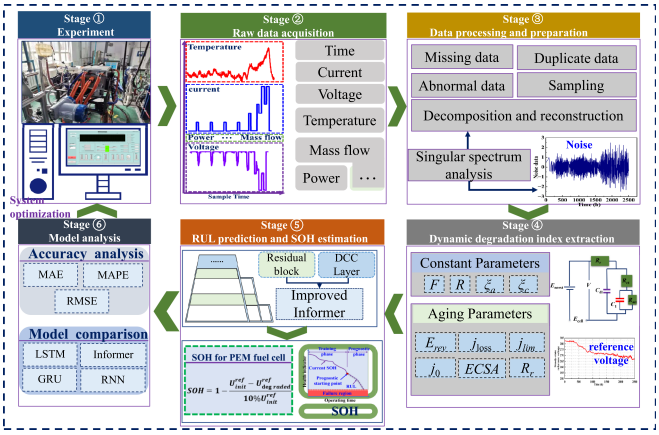

Fig. 4. Proposed framework for degradation prediction and SOH estimation for vehicular FCSs based on the improved Informer model.

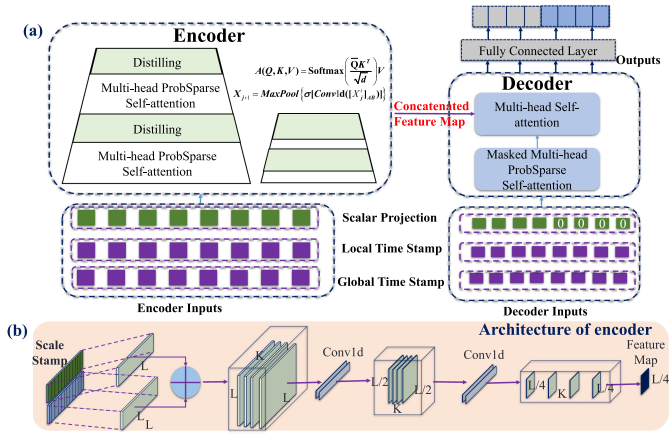

Fig. 5. Architecture of the Informer model.

model described above has the ability to characterize the dynamic performance of the fuel cells under different degradation levels.

IV. Fusion Prognostic Strategy

After obtaining the current degradation characteristics of the vehicular FCS, the voltage degradation trend or SOH of FCSs needs to be further predicted. In this section, we introduce an improved Informer model architecture designed for long-term prognostics of degradation characteristics under dynamic operating cycles, as illustrated in Fig. 4.

Within this framework, the long-term aging prediction of the FCS is delineated through six stages. First, a durability test is conducted, yielding corresponding durability data. Subsequently, the raw data obtained from this test are processed and reconstructed based on the singular spectrum analysis method. Following this, dynamic degradation characteristics are extracted, and the virtual steady-state reference voltage is obtained by using the equivalent circuit model presented in this article. Finally, the current SOH estimation and voltage degradation prediction, along with the corresponding accuracy analysis, are performed.

A. Improved Informer Architecture for the Degradation Prediction

The Informer network represents an improved algorithm rooted in Transformer architecture. Its refined probabilistic sparse self-attention mechanism accurately captures the long-term dependencies of time series data and fully exploits the temporal correlation of degradation indexes [47]. The unique encoder–decoder structure of the Informer neural network solves the memory degradation issue associated with lengthy series in traditional methods and improves the accuracy of long-term voltage degradation prediction of the FCS. The architecture of the Informer neural network is illustrated in Fig. 5.

As shown in Fig. 5, the encoder is internally stacked with multihead ProbSparse self-attention modules and "distilling" mechanisms, and the encoder is mainly used to capture the long-term dependence of the voltage degradation data for the vehicular FCS and send the part of historical voltage degradation data to multihead sparse self-attention module. The probabilistic sparse self-attention mechanism is calculated as follows:

$$A(Q,K,V) = \text{Softmax}\left(\frac{\overline{Q}K^T}{\sqrt{d}}\right)V \tag{23}$$

where $Q \in \mathbb{R}^{L_Q \times d_{model}}$, $K \in \mathbb{R}^{L_k \times d_{model}}$, and $V \in \mathbb{R}^{L_V \times d_{model}}$, which are obtained by a linear transformation of voltage degradation data. $\overline{Q}$is the sparse matrix, and Q becomes $\overline{Q}$after probability sparse operation.

Although the Informer neural network has a strong ability to capture extensive sequence information, outperforming existing mainstream prediction models, certain limitations arise when applied to the long-term degradation data of FCSs in this study. In the encode module of the Informer model, although the distilling operation between each two self-attention blocks can further reduce memory usage, the cumulative effect of stacking these blocks with distillation may not yield sufficient benefits as computing costs increase. Instead, it could cause repetitive and meaningless computation because of a constrained receptive field. In addition, the distilling operation lacks consideration for temporal perspective, introducing the risk of future information leakage in time series forecasting. Therefore, to better apply the Informer model to the prediction of long-term decay characteristics of fuel cells in this article, a further refinement is applied to the encode module, as depicted in Fig. 6. This improved solution is inspired by the work of Bai et al. [48] Specifically, the dilated causal convolution in the encoder module is used instead of the "distilling" operation to obtain an exponentially receptive field growth. In fact, when a canonical convolution is applied to the time series prediction task of predicting long-period fuel cell voltage degradation, it is only able to look back linear-size history as the depth of the network grows. However, the dilated causal convolution can flexibly adjust the model receptive field by selecting filters of different sizes or adding dilatation factors so that the top-level output can receive a wider range of input information, thereby improving the ability of causal convolution to model longer input sequences. For a 1-D sequence, input

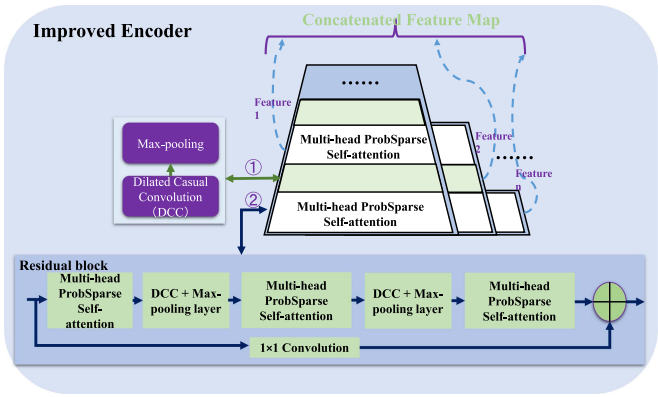

Fig. 6. Improved encode module for the Informer neural network.

$\mathbf{x} \in \mathbb{R}^n$ and a filter $f : \{0, \ldots, k-1\} \to \mathbb{R}$, the dilated convolution operation F on an element s of the sequence is defined as

$$F(s) = (\mathbf{x} *_d f)(s) = \sum_{i=0}^{k-1} f(i) \cdot \mathbf{x}_{s-d \cdot i} \tag{24}$$

where d is the dilation factor, $k$is the filter size, and $s - d \cdot i$ accounts for the direction of the past.

In addition, while incorporating multiple self-attention blocks and convolution blocks is beneficial for extracting profound feature maps, the escalating depth of the network introduces a challenge. With each layer, there is a diminishing return in the information captured, leading to the potential issue of gradient vanishing. To address this issue, the residual block is added to the encode module to maintain diversity in extracting information related to fuel cell decay characteristics, thereby accelerating model convergence, as shown in Fig. 6. Within a residual block, the output of the first multihead ProbSparse self-attention block is fused with the output of the third attention block. As 1×1 convolution is used to ensure uniformity in the shape of the feature maps from the outputs of the two attention blocks.

V. Experiment Validation

A. Dynamic Degradation Characteristics Analysis of the Fuel Cell Stack

According to the ECM constructed in Section III that characterizes the dynamic decay behavior of the FCS, the degradation behavior parameters such as R_r, R_{ct}, R_{mt}, and C_{dl} can be identified, and the changes of corresponding parameters in the dynamic durability test over 2500 h are shown in Fig. 7.

It can be seen from Fig. 7 that as the FCS continues to operate under dynamic load cycles, the aging parameters (R_r, R_{ct}, and R_{mt}) show a discernible periodic fluctuation with an overall increasing trend. Before the durability test, R_r, R_{mt}, and R_{ct} of the fuel cell stack are 0.639, 0.817, and 0.912 $m\Omega$, respectively. After the durability test over 2500 h, R_r, R_{mt}, and, R_{ct} of the FCS increased to 1.236, 0.921, and 1.096 $m\Omega$, respectively, i.e., increase by 93.3%, 12.6%, and 20.2%. It implied that the transfer process of charge and mass is inhibited, which is closely related to the structural damage of MEA. The structural damage of the

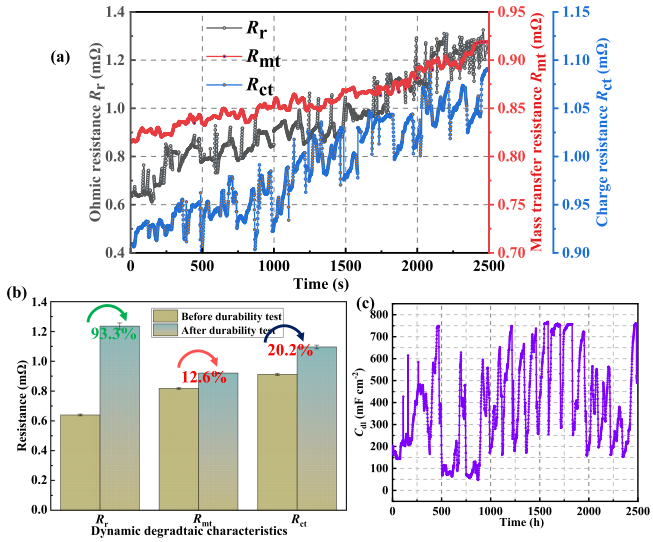

Fig. 7. Degradation characteristics parameters of FCSs. (a) Change curves of degradation characteristic parameters R_r, R_{ct}, $R_{mt}$with durability time. (b) Growth ratio of the degradation characteristic parameters R_r, R_{ct}, R_{mt}. (c) Change curves of dynamic characteristic parameters C_{dl} with durability time.

CL could result in an increasing resistance. Following the durability test, there was a notable increase in the surface roughness of both the anodic and cathodic CLs. This increase may potentially harm the pore structure, causing loss and agglomeration of catalysts. As a result, this negatively impacts the Pt/C catalytic activity, resulting in an augmented activation loss. In addition, the long-term durability test of FCSs under vehicle conditions may lead to the excessive coverage of Pt/C catalyst particles by polymers. This, in turn, may cause the destruction of the carbon carrier structure and the formation of oxygen-containing groups. These changes restrict the transmission of hydrogen and oxygen, causing an increase in mass transfer loss for PEM fuel cells. Fig. 7(c) describes the change of double-layer capacitance under dynamic operational conditions. The trend characteristics C_{dl} are not readily apparent during transient loading and unloading. This observation is pivotal for establishing the virtual reference steady-state voltage, which will be discussed in Section V-B.

According to (4), to accurately characterize the voltage variation of FCSs under dynamic cycling, j_{loss}, j_{lim}, and j_0 need to be further calculated. In this article, combining (4) and the polarization curves of the FCS at different decay stages, the decay factors j_{loss}, j_{lim}, and $j_0$can be accurately identified, as shown in Fig. 8(b)–(d).

B. Virtual Steady-State Voltage Results

Since the final output of the degradation mechanism model proposed in this article is the stack voltage, so according to Chinese National Standard [36], the SOH of the FCS can be defined as

$$\mathrm{SOH} = 1 - \frac{U_{\mathrm{init}}^{\mathrm{ref}} - U_{\mathrm{degraded}}^{\mathrm{ref}}}{10\% U_{\mathrm{init}}^{\mathrm{ref}}} \tag{25}$$

where $U_{\mathrm{init}}^{\mathrm{ref}}$ is the stack voltage of fresh fuel cells at the reference current; $U_{\mathrm{degraded}}^{\mathrm{ref}}$ is the degraded voltage at the reference current,

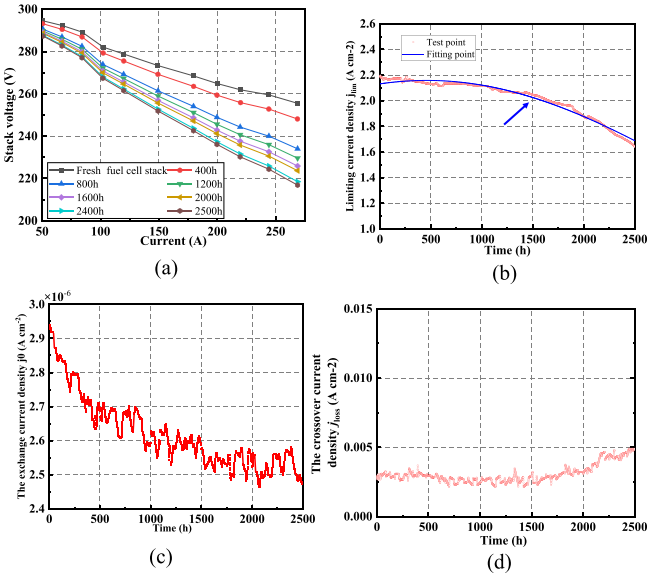

Fig. 8. Polarization curves of the PEM fuel cell under different decay stages and Change curves of degradation-related parameters j_{loss}, j_{lim}, and j_0 with durability time (a) polarization curves. (b) Limiting current density (j_{lim}). (c) Exchange current density (j_0). (d) Crossover current density.

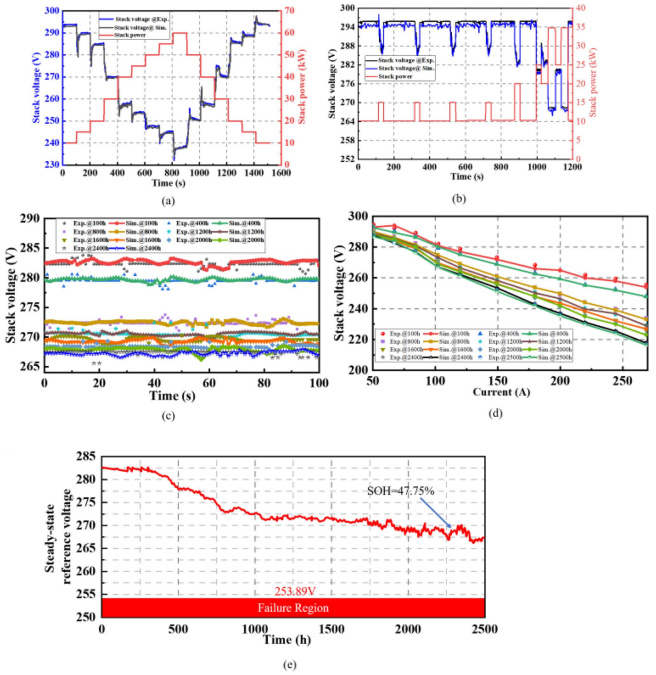

Fig. 9. Accuracy verification results of the proposed dynamic degradation model for FCSs. (a) Dynamic operation cycle verification. (b) Durability test cycle verification. (c) Steady-state reference voltage verification under different test periods. (d) Polarization curve verification under the different degradation levels. (e) Variation of the estimated virtual steady-state reference voltage.

which can be calculated by introducing all identified parameters into (5) and setting the operating current at 102 A.

According to (25), to accurately estimate the current SOH of FCSs and perform subsequent voltage degradation trend predictions, it is crucial to accurately calculate $U^{\text{ref}}_{\text{degraded}}$ over time. In this section, we first verify the accuracy of the time-varying dynamic degradation model established by integrating the aging parameters and dynamic characteristic parameters obtained from Figs. 7 and 8. The corresponding accuracy verification results of external characteristics for FCSs are presented in Fig. 9. Specifically, as shown in Fig. 9(a) and (b), it is validated that the proposed time-varying dynamic degradation model can effectively simulate the changes in FCSs under different current loads, especially during moments of abrupt current switching. Furthermore, Fig. 9(c) and (d) exhibits a precise comparison of virtual steady-state voltage variations and polarization curves at different stages of the durability test. This illustrates the effectiveness of the proposed methodology in using the ECM to characterize the dynamic behavior of the fuel cell stack and characterize the virtual reference steady-state voltage at various levels of SOH. In addition, the virtual reference voltage $U^{\text{ref}}_{\text{degraded}}$ at the reference current of 102 A throughout the 2500 h durability test is calculated based on the proposed time-varying dynamic degradation model, as shown in Fig. 9(e). The figure illustrates that the performance of the fuel cell stack undergoes increasingly severe degradation over time, aligning with intuitive analysis. The reference voltage decreases from 282.11 V to 267.37 V, corresponding to a 52.25% decline in SOH.

C. Long-Term Aging Prediction Results

After obtaining the virtual steady-state reference voltage of the whole durability test, it is one of the most critical steps to use the improved Informer model to predict voltage degradation and evaluate its accurate performance. In this article, some hyperparameters of the improved Informer model when performing voltage degradation tasks are shown in Table II.

TABLE II
MODEL HYPERPARAMETERS OF THE IMPROVED INFORMER

Hyperparameters	Values
Initial learning rate	0.0001
Dropout	0.05
Regularization	0.00001
Test data percentage	60%,50%,40%,30%
Optimizer	Adam
Sliding window length	15
Train data percentage	40%,50%,60%,70%

1) Long-Term Aging Prediction Results Using the Improved Informer Model: To assess the efficacy and accuracy of the improved Informer model proposed for predicting the long-term aging of FCSs, the prediction results of the FCS aging under 40% (400 h), 50% (500 h), 60% (600 h), and 70% (700 h) training sets are investigated, as shown in Fig. 10(a)–(d).

Fig. 10 illustrates that the enhanced Informer model, as proposed, adeptly forecasts both the prolonged aging trajectory and voltage cyclic recovery of FCSs. Specifically, when predicting the future 300 h–700 h decay trend of the reference voltage, the root-mean-square error (RMSE) for the proposed model falls within the range of 0.33–1.04 V, and the mean absolute percentage error (MAPE) is less than 0.5%. These results signify

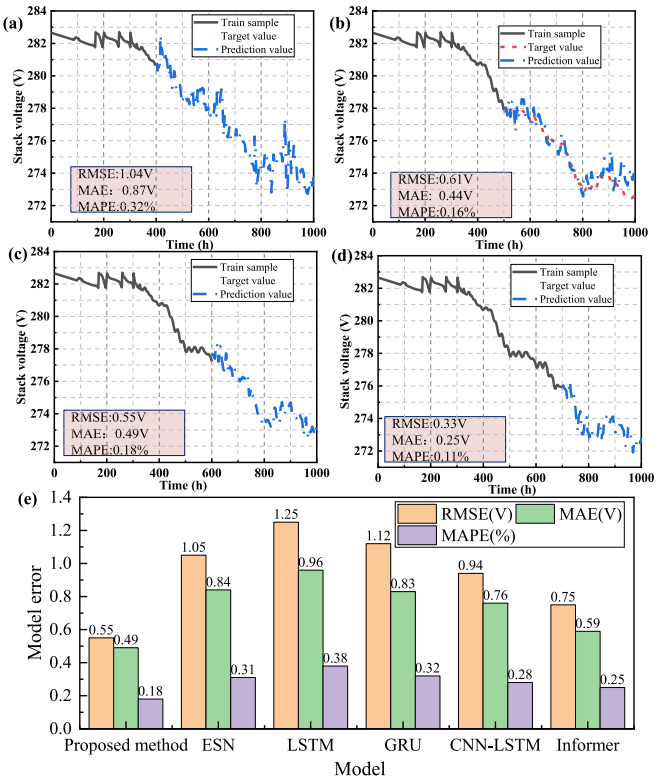

Fig. 10. Aging prediction results using the improved Informer model. (a)–(d) Prediction results of the stack voltage under different training datasets. (e) Model error analysis.

TABLE III
MODEL HYPERPARAMETERS OF THE COMPARISON MODELS

Model	Hyperparameters	Values
ESN	Reservoir size	50
	Spectral radius	1
	Regularization	0.01
LSTM/GRU/CNN-LSTM	Leakage rate	0.2
	Learning rate	0.001
	Batch size	128
	Iteration	800
	Dropout	0.1
	Hidden unit	12

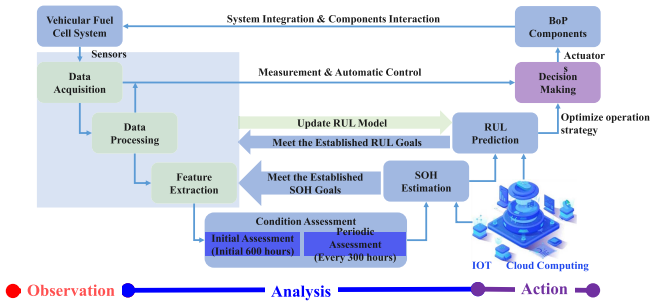

Fig. 11. Rolling prediction framework for vehicular FCSs.

the commendable long-term degradation prediction capabilities of the proposed Informer model. Moreover, within the initial 600 h training set of the rolling prediction framework presented in Section V-C.(2), the RMSE, mean absolute error (MAE), and MAPE of the improved Informer model are 0.55 V, 0.49 V, and 0.18%, respectively. These outcomes lay a robust foundation for the establishment of the rolling prediction framework aimed at prolonging the lifetime of vehicular FCSs. To further underscore the superiority of the proposed method regarding accuracy, several common models, including echo state networks (ESN), long short-term memory (LSTM), gate recurrent unit (GRU), convolutional neural networks (CNN)-LSTM, and the original Informer model, are selected for a comparative analysis. The model hyperparameters of the comparison models are listed in Table III. The evaluation results of model performance, depicted in Fig. 10(e), manifest a clear accuracy advantage for the improved Informer in long-term degradation prediction, indicating that the improved Informer model is more suitable for the rolling prediction framework designed for optimizing the lifespan of vehicular FCSs in cloud-based applications, as illustrated in the following section.

2) Rolling Prediction Framework Applicable in Cloud-Based Applications: Stimulated by the rapid development of cloud technologies and intelligent transportation systems [43], it is expected that SOH estimation and degradation prediction technologies for vehicular FCS can be upgraded through the Internet of Things and cloud computing technologies. Therefore, a rolling prediction framework applicable in Cloud-Based SOH estimation of FCSs based on the improved Informer model is proposed, as illustrated in Fig. 11.

As indicated in Fig. 11, in the proposed rolling prediction framework, first, a completely new fuel cell stack is operated for hundreds of hours (600 h in this article) under the established control strategy and operation cycle, and then the initial degradation prediction model from the cloud is trained according to the operation data collected by the onboard sensors and the models developed in Sections III and IV to determine SOH level under the current operation strategy. If the current SOH level of the FCS meets the established goals, the vehicular FCS continues to operate according to the previous operation strategy, and new operating data is added to the training dataset to improve the predictive accuracy of the voltage degradation prediction model; otherwise, the control strategy and operating parameters of the vehicular FCS system need to be further optimized using the over the air technology from cloud, such as cathode and anode inlet pressure, operating temperature, and oxygen excess ratio control. In particular, in this article, after the initial voltage degradation prediction model is trained, the data collected from the onboard sensor will be updated every 300 h into the proposed long-term aging prediction model to continuously improve the accuracy and generalization ability of the model. The long-term degradation prognostic results of the vehicular FCS obtained according to the proposed optimal lifetime prediction framework are illustrated in Fig. 12.

Fig. 12 shows the prediction results of the rolling prediction framework. Within each rolling prediction period, the mean

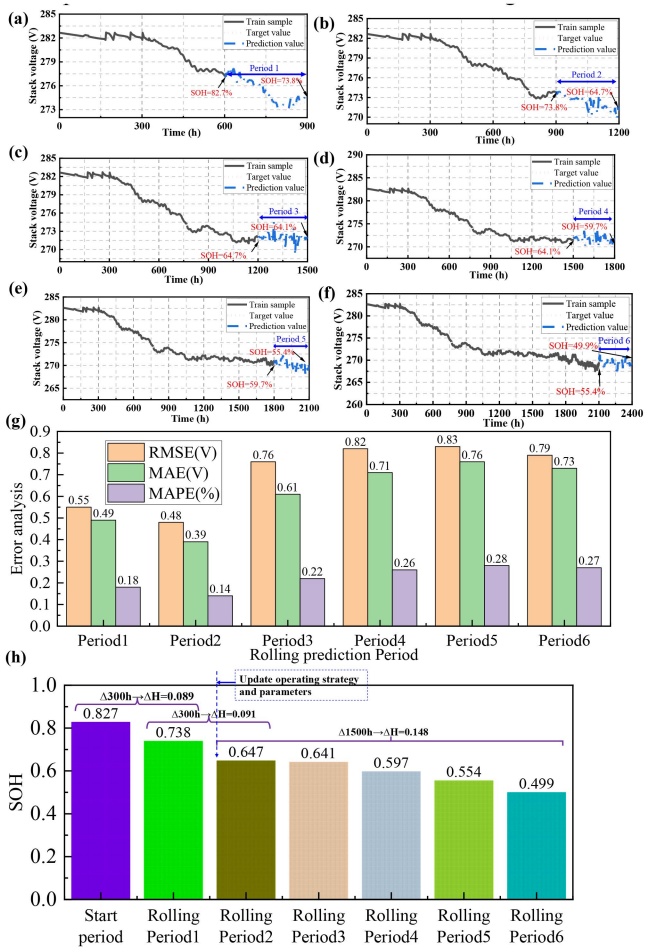

Fig. 12. Durability prediction results using the proposed rolling prediction framework. (a)–(f) Prediction results of the stack voltage under different rolling prediction periods. (g) Error analysis. (h) SOH changes under the rolling prediction framework.

values for RMSE, MAE, and MAPE associated with the reference voltage prediction are 0.705 V, 0.615 V, and 0.225 V, respectively. The corresponding maximum values are 0.83 V, 0.76 V, and 0.28 V, indicating that the proposed model accurately captures the overall degradation trend in each period. In addition, as indicated in Fig. 12(h), the SOH of the FCS decreases from 100% to 82.7% during the initial 600-h durability test. Utilizing the current operation strategy, the predicted SOH values for the 900th and 1200th hour, obtained through the rolling prediction framework, are 73.8% and 64.7%, respectively. These represent decreases of 8.89% and 9.1%, falling short of the durability target. Therefore, the operation parameters are adjusted at the 1200th hour. The subsequent SOH predictions after 1800, 2100, and 2400 h are 59.7%, 55.4%, and 49.9%, respectively, corresponding to the reductions in SOH by just 4.4%, 4.3%, and 5.5% at each test interval. These quantitative evaluations offer valuable insights into the design, integration, control strategy, and operation parameters of current vehicular FCS systems and components. In conclusion, the durability prediction framework proposed in this article serves as a valuable guide for designing fuel cell systems and formulating control strategies. This framework significantly reduces development cycles and costs and contributes to both theoretical innovation and practical engineering applications.

VI. Conclusion

To establish a reliable long-term estimation and prognosis for the SOH and voltage degradation of vehicular FCSs, a fusion prognostic strategy that uses an ECM to extract dynamic degradation features and an improved Informer model for SOH estimation and degradation prediction is proposed. Subsequently, this article introduces a novel rolling prediction framework for SOH estimation of FCSs designed for cloud-based applications, building upon the improved Informer model. The key conclusions drawn from this research are as follows.

1) The constructed time-varying dynamic degradation model based on the electrochemical mechanism and dynamic ECM can effectively capture the dynamic degradation behavior of FCSs. The dynamic degradation characteristic R_{r}, R_{ct}, R_{mt}, j_{loss}, j_0, and j_{lim} can be obtained in real time. Moreover, after a 2500-h durability test, the reference voltage decreases from 282.11 V to 267.37 V, corresponding to a 52.25% decline in SOH; The R_{r}, R_{mt}, and R_{ct} of the FCS exhibited significant increases of 93.3%, 12.6%, and 20.2%, respectively.
2) The improved Informer model proposed demonstrates a distinct accuracy advantage in long-term SOH estimation tasks. It excels in accurately predicting both the extended aging trend and the periodic voltage recovery of FCSs, which outperform other data-driven methods, such as ESN, LSTM, GRU, CNN-LSTM, and the original Informer model.
3) The proposed rolling prediction for extending the lifespan of vehicular FCSs in a cloud environment offers quantitative SOH evaluation values for each operational period, operation strategy, or parameter. This framework serves as a valuable guide for designing fuel cell systems and formulating control strategies.

References

[1] K. Jiao et al., "Designing the next generation of proton-exchange membrane fuel cells," *Nature*, vol. 595, pp. 361–369, 2021, doi: 10.1038/s41586-021-03482-7.
[2] Y. Qiu et al., "Progress and challenges in multi-stack fuel cell system for high power applications: Architecture and energy management," *Green Energy Intell. Transp.*, vol. 2, no. 2, 2023, Art. no. 100068, doi: 10.1016/j.geits.2023.100068.
[3] Y. Sun et al., "Advancements in cathode catalyst and cathode layer design for proton exchange membrane fuel cells," *Nature Commun.*, vol. 12, 2021, Art. no. 5984, doi: 10.1038/s41467-021-25911-x.
[4] S. Zhou, S. Jin, X. Liu, H. Bai, Y. Huangfu, and F. Gao, "Robust voltage control with resonant extended state observer for hybrid fuel cell system," *IEEE Trans. Power Electron.*, vol. 39, no. 5, pp. 5462–5472, May 2024, doi: 10.1109/TPEL.2024.3367907.
[5] J. Jin, Y. Chen, C. Xie, and F. Wu, "Degradation prediction of PEMFC based on data-driven method with adaptive fuzzy sampling," *IEEE Trans. Transp. Electrific.*, vol. 10, no. 2, pp. 3363–3372, Jun. 2024, doi: 10.1109/TTE.2023.3296719.
[6] X. Tang, Y. Zhang, and S. Xu, "Temperature sensitivity characteristics of PEM fuel cell and output performance improvement based on optimal active temperature control," *Int. J. Heat Mass Transfer*, vol. 206, 2023, Art. no. 123966, doi: 10.1016/j.ijheatmasstransfer.2023.123966.

[7] W. Xue, X. Zhang, L. Sun, and H. Fang, "Extended state filter based disturbance and uncertainty mitigation for nonlinear uncertain systems with application to fuel cell temperature control," *IEEE Trans. Ind. Electron.*, vol. 67, no. 12, pp. 10682–10692, Dec. 2020, doi: 10.1109/TIE.2019.2962426.

[8] C. Wang et al., "A fusion prognostic strategy for fuel cells operating under dynamic conditions," *eTransportation*, vol. 12, 2022, Art. no. 100166, doi: 10.1016/j.etran.2022.100166.

[9] T. Ramsden, "2019 Annual progress report: DOE hydrogen and fuel cells program," United States, 2020. [Online]. Available: https://www.osti.gov/biblio/1660255

[10] K. Chen, S. Laghrouche, and A. Djerdir, "Prognosis of fuel cell degradation under different applications using wavelet analysis and nonlinear autoregressive exogenous neural network," *Renewable Energy*, vol. 179, pp. 802–814, 2021, doi: 10.1016/j.renene.2021.07.097.

[11] E. Wallnöfer-Ogris et al., "Main degradation mechanisms of polymer electrolyte membrane fuel cell stacks – Mechanisms, influencing factors, consequences, and mitigation strategies," *Int. J. Hydrogen Energy*, vol. 50, pp. 1159–1182, 2024, doi: 10.1016/j.ijhydene.2023.06.215.

[12] C. Zhang et al., "A health management review of proton exchange membrane fuel cell for electric vehicles: Failure mechanisms, diagnosis techniques and mitigation measures," *Renewable Sustain. Energy Rev.*, vol. 182, 2023, Art. no. 113369, doi: 10.1016/j.rser.2023.113369.

[13] S. Dirkes et al., "Prescriptive lifetime management for PEM fuel cell systems in transportation applications, part II: On-board operando feature extraction, condition assessment and lifetime prediction," *Energy Convers. Manage.*, vol. 283, 2023, Art. no. 116943, doi: 10.1016/j.enconman.2023.116943.

[14] Y. Liu, M. Li, Y. Wang, Z. Sun, and Z. Chen, "Predictive energy management for fuel cell hybrid vehicles considering efficiency and safety," *IEEE Trans. Power Electron.*, vol. 39, no. 10, pp. 13842–13852, Oct. 2024, doi: 10.1109/TPEL.2024.3422679.

[15] R. Song, X. Liu, Z. Wei, F. Pan, Y. Wang, and H. He, "Safety and longevity-enhanced energy management of fuel cell hybrid electric vehicle with machine learning approach," *IEEE Trans. Transp. Electrific.*, vol. 10, no. 2, pp. 2562–2571, Jun. 2024, doi: 10.1109/TTE.2023.3295433.

[16] C. Jia, W. Qiao, J. Cui, and L. Qu, "Adaptive model-predictive-control-based real-time energy management of fuel cell hybrid electric vehicles," *IEEE Trans. Power Electron.*, vol. 38, no. 2, pp. 2681–2694, Feb. 2023, doi: 10.1109/TPEL.2022.3214782.

[17] X. Hu, C. Zou, X. Tang, T. Liu, and L. Hu, "Cost-optimal energy management of hybrid electric vehicles using fuel/battery health-aware predictive control," *IEEE Trans. Power Electron.*, vol. 35, no. 1, pp. 382–392, Jan. 2020, doi: 10.1109/TPEL.2019.2915675.

[18] Z. Tian et al., "A novel aging prediction method of fuel cell based on empirical mode decomposition and complexity threshold quantitative criterion," *J. Power Sources*, vol. 574, 2023, Art. no. 233120, doi: 10.1016/j.jpowsour.2023.233120.

[19] H. Wu, W. Wang, Y. Li, W. Zhu, C. Xie, and H. B. Gooi, "Hybrid physics-based and data-driven prognostic for PEM fuel cells considering voltage recovery," *IEEE Trans. Energy Convers.*, vol. 39, no. 1, pp. 601–612, Mar. 2024, doi: 10.1109/TEC.2023.3311460.

[20] W. Huang et al., "Life prediction for proton exchange membrane fuel cell based on experimental results and combinatorial optimization algorithm," *Int. J. Hydrogen Energy*, vol. 79, pp. 364–376, 2024, doi: 10.1016/j.ijhydene.2024.07.029.

[21] Y. Xu, C. Jiang, J. Peng, X.-L. Wu, L. Xiao, and X. Li, "Fault prognosis method for solid oxide fuel cells based on mechanism degradation process model and particle filtering," *IEEE Trans. Power Electron.*, vol. 38, no. 6, pp. 6831–6840, Jun. 2023, doi: 10.1109/TPEL.2023.3246068.

[22] W. Ming, P. Sun, and Z. Zhang, "A systematic review of machine learning methods applied to fuel cells in performance evaluation, durability prediction, and application monitoring," *Int. J. Hydrogen Energy*, vol. 48, no. 13, pp. 5197–5228, 2023, doi: 10.1016/j.ijhydene.2022.10.261.

[23] X. Tang et al., "A novel online degradation model for proton exchange membrane fuel cell based on online transfer learning," *Int. J. Hydrogen Energy*, vol. 48, no. 36, pp. 13617–13632, 2023, doi: 10.1016/j.ijhydene.2022.12.260.

[24] K. Chen, S. Laghrouche, and A. Djerdir, "Fuel cell health prognosis using unscented kalman filter: Postal fuel cell electric vehicles case study," *Int. J. Hydrogen Energy*, vol. 44, no. 3, pp. 1930–1939, 2019, doi: 10.1016/j.ijhydene.2018.11.100.

[25] M. Ou et al., "A novel approach based on semi-empirical model for degradation prediction of fuel cells," *J. Power Sources*, vol. 488, 2021, Art. no. 229435, doi: 10.1016/j.jpowsour.2020.229435.

[26] G. A. Futter, A. Latz, and T. Jahnke, "Physical modeling of chemical membrane degradation in polymer electrolyte membrane fuel cells: Influence of pressure, relative humidity and cell voltage," *J. Power Sources*, vol. 410/411, pp. 78–90, 2019, doi: 10.1016/j.jpowsour.2018.10.085.

[27] Y. Wang et al., "Degradation prediction of proton exchange membrane fuel cell stack using semi-empirical and data-driven methods," *Energy AI*, vol. 305, 2022, Art. no. 117735, doi: 10.1016/j.apenergy.2021.117735.

[28] K. Benaggoune et al., "A data-driven method for multi-step-ahead prediction and long-term prognostics of proton exchange membrane fuel cell," *Appl. Energy*, vol. 313, 2022, Art. no. 118835, doi: 10.1016/j.apenergy.2022.118835.

[29] B. Sun et al., "Short-term performance degradation prediction of a commercial vehicle fuel cell system based on CNN and LSTM hybrid neural network," *Int. J. Hydrogen Energy*, vol. 48, no. 23, pp. 8613–8628, 2023, doi: 10.1016/j.ijhydene.2022.12.005.

[30] Z. Hua, Z. Zheng, E. Pahon, M.-C. Péra, and F. Gao, "Lifespan prediction for proton exchange membrane fuel cells based on wavelet transform and echo State network," *IEEE Trans. Transp. Electrific.*, vol. 8, no. 1, pp. 420–431, Mar. 2022, doi: 10.1109/TTE.2021.3121179.

[31] Z. Hua et al., "Remaining useful life prediction of PEMFC systems based on the multi-input echo state network," *Appl. Energy*, vol. 265, 2020, Art. no. 114791, doi: 10.1016/j.apenergy.2020.114791.

[32] J. Zuo et al., "Deep learning based prognostic framework towards proton exchange membrane fuel cell for automotive application," *Appl. Energy*, vol. 281, 2021, Art. no. 115937, doi: 10.1016/j.apenergy.2020.115937.

[33] Z. Lyu, Y. Wang, and A. Sciazko, "Prediction of fuel cell performance degradation using a combined approach of machine learning and impedance spectroscopy," *J. Energy Chem.*, vol. 87, pp. 32–41, 2023, doi: 10.1016/j.jechem.2023.08.028.

[34] J. Lv, Z. Yu, H. Zhang, G. Sun, P. Muhl, and J. Liu, "Transformer based long-term prognostics for dynamic operating PEM fuel cells," *IEEE Trans. Transp. Electrific.*, vol. 10, no. 1, pp. 1747–1747, Mar. 2024, doi: 10.1109/TTE.2023.3266803.

[35] R. Pan et al., "Performance degradation prediction of proton exchange membrane fuel cell using a hybrid prognostic approach," *Int. J. Hydrogen Energy*, vol. 45, no. 55, pp. 30994–31008, 2020, doi: 10.1016/j.ijhydene.2020.08.082.

[36] R. Ma, R. Xie, L. Xu, Y. Huangfu, and Y. Li, "A hybrid prognostic method for PEMFC with aging parameter prediction," *IEEE Trans. Transp. Electrific.*, vol. 7, no. 4, pp. 2318–2331, Dec. 2021, doi: 10.1109/TTE.2021.3075531.

[37] X. Tang et al., "Adaptive state-of-health temperature sensitivity characteristics for durability improvement of PEM fuel cells," *Chem. Eng. J.*, vol. 491, 2024, Art. no. 151951, doi: 10.1016/j.cej.2024.151951.

[38] H. Liu et al., "Remaining useful life estimation for proton exchange membrane fuel cells using a hybrid method," *Appl. Energy*, vol. 237, pp. 910–919, 2019, doi: 10.1016/j.apenergy.2019.01.023.

[39] J. Liu, E. Zio, and Y. Hu, "Particle filtering for prognostics of a newly designed product with a new parameter initialization strategy based on reliability test data," *IEEE Access*, vol. 6, pp. 62564–62573, 2018, doi: 10.1109/ACCESS.2018.2876457.

[40] R. Xie et al., "Prognostic for fuel cell based on particle filter and recurrent neural network fusion structure," *Energy AI*, vol. 2, 2020, Art. no. 2100017, doi: 10.1016/j.egyai.2020.100017.

[41] Gb/T 38914-2020, "Evaluation method for lifetime of proton exchange membrane fuel cell stack in vehicle application," 2020. [Online]. Available: https://openstd.samr.gov.cn/bzgk/gb/index

[42] Z. Bao et al., "High-consistency proton exchange membrane fuel cells enabled by oxygen-electron mixed- pathway electrodes via digitalization design," *Sci. Bull.*, vol. 68, pp. 266–275, 2023, doi: 10.1016/j.scib.2023.01.034.

[43] Y. Qin et al., "Experiment investigation of the dynamic characteristic and performance improvement of kW-grade air cooled fuel cells," *Energy Convers. Manage.*, vol. 310, 2024, Art. no. 118440, doi: 10.1016/j.enconman.2024.118440.

[44] H. Chaoui, M. Kandidayeni, L. Boulon, S. Kelouwani, and H. Gualous, "Real-time parameter estimation of a fuel cell for remaining useful life assessment," *IEEE Trans. Power Electron.*, vol. 36, no. 7, pp. 7470–7479, Jul. 2021, doi: 10.1109/TPEL.2020.3044216.

[45] H. Yuan et al., "Understanding dynamic behavior of proton exchange membrane fuel cell in the view of internal dynamics based on impedance," *Chem. Eng. J.*, vol. 431, 2022, Art. no. 134035, doi: 10.1016/j.cej.2021.134035.

[46] C. S. Spiegel, *Designing & Building Fuel Cells[M]*. New York, NY, USA: McGraw-Hill, 2007, pp. 1–7.
[47] H. Zhou et al., "Informer: Beyond efficient transformer for long sequence time-series forecasting," in *Proc. 35th AAAI Conf. Artif. Intell.*, 2021, pp. 11106–11115, doi: 10.1609/aaai.v35i12.17325.
[48] S. Bai, Z. Kolter, and V. Koltun, "An empirical evaluation of generic convolutional and recurrent networks for sequence modeling," 2018, *arXiv:1803.01271*, doi: 10.48550/arXiv.1803.01271.

Xingwang Tang received the M.S. degree in power engineering from the Jilin University, Changchun, China, in 2021. He is currently working toward the Ph.D. degree in energy and power engineering with School of Automotive Studies, Tongji University, Shanghai, China.

From 2023 to 2024, he is a visiting research scholar with the Department of Mechanical Engineering, National University of Singapore, Singapore. His current research interests include modeling, durability control, energy management strategy, and state-of health estimation for vehicular fuel cell systems.

Lei Shi received the M.S. degree in vehicle engineering from the Shandong Jianzhu University, Jinan, China, in 2019 and the Ph.D. degree in energy and power engineering from the Tongji University, Shanghai, China, in 2024.

He is currently a Postdoctor with the School of Automotive Studies, Tongji University. His current research interests include modeling, cold start, water-heat transfer mechanism, and durability control for fuel cell systems.

Ming Li received the B.E., M.S., and Ph.D. degrees in power machinery and engineering from the Jilin University, Changchun, China, in 2000, 2003, and 2007, respectively.

He is currently a Professor with the College of Automotive Engineering, Jilin University. His current research interests include fuel cells and lithium batteries for large-scale energy storage applications, as well as their thermal design, optimization, and modelling study.

Sichuan Xu received the B.E. degree in power machinery and engineering from the Tongji University, Shanghai, China, in 1984, and the M.S. and Ph.D. degrees in power machinery and engineering from the Jilin University, Changchun, China, in 1987 and 1996, respectively.

He is currently a Professor with the School of Automotive Studies, Tongji University. His research interests include design and control of fuel cell systems, as well as electrical power conversion for fuel cell vehicles.

Chuanyu Sun (Member, IEEE) received the bachelor's degree in material chemistry from Tianjin University, Shanghai, China, in 2012, the master's degree in materials science and nanotechnology from Politecnico Di Milano Milan, Italy, in 2014, and the Doctor degree in materials science and Nanostructure from Università degli Studi di Padova, Padua, Italy, 2019.

He has been an Associate Professor with the School of Electrical Engineering and Automation, Harbin Institute of Technology, Harbin, China, since Oct. 2022. His current research interests include fuel cells and redox flow batteries for large-scale energy storage applications, as well as their design, optimization, and modelling study.